J Therm Anal Calorim (2010) 102:23–29
DOI 10.1007/s10973-009-0338-3

Thermal decomposition behavior of potassium and sodium jarosite synthesized in the presence of methylamine and alanine

J. Michelle Kotler · Nancy W. Hinman · C. Doc Richardson · Jill R. Scott

Received: 19 May 2009 / Accepted: 3 July 2009 / Published online: 28 August 2009

Abstract Biomolecules, methylamine and alanine, found associated with natural jarosite samples peaked the interest of astrobiologists and planetary geologists. How the biomolecules are associated with jarosite remains unclear although the mechanism could be important for detecting biosignatures in the rock record on Earth and other planets. A series of thermal gravimetric experiments using synthetic K-jarosite and Na-jarosite were conducted to determine if thermal analysis could differentiate physical mixtures of alanine and methylamine with jarosite from samples where the methylamine or alanine was incorporated into the synthesis procedure. Physical mixtures and synthetic experiments with methylamine and alanine could be differentiated from one another and from the standards by thermal analysis for both the K-jarosite and Na-jarosite end-member suites. Changes included shifts in on-set temperatures, total temperature changes from on-set to final, and the presence of indicator peaks for methylamine and alanine in the physical mixture experiments.

J. M. Kotler · N. W. Hinman (✉) · C. D. Richardson
Geosciences Department, University of Montana,
Missoula, MT 59812, USA
e-mail: nancy.hinman@umontana.edu

J. M. Kotler
e-mail: julia.kotler@umontana.edu

Present Address:
J. M. Kotler
North American Palladium, Metals Exploration Division,
556 Tenth Avenue, Thunder Bay, ON P7B 2R2, Canada
e-mail: mkotler@napalladium.com

J. R. Scott
Chemical Sciences, Idaho National Laboratory,
Idaho Falls, ID 83415, USA

Keywords Jarosite · Mars · Methylamine · Alanine · Biosignatures

Introduction

Jarosite ($KFe_3(SO_4)_2(OH)_6$) was found on Mars in 2004 by the Mars Exploration Rover mission [1] after first being proposed for the martian surface in the late 1980s by Burns [2, 3]. The mineral group is associated with biologic activity on Earth; microbes oxidize both iron and sulfur in primary minerals for energy, forming jarosite as a by-product [4, 5]. The same primary iron and sulfur minerals (pyrrhotite, marcasite, and pyrite) associated with jarosite on Earth are inferred to occur on Mars [2, 3, 6–13]. The chemical and physical properties of the mineral could allow biomolecules left over from biogenic formation to be incorporated into the crystal structure and serve as potential biosignatures [14]. Several analytical techniques have identified biomolecules, such as amino acids and amino acid degradation products, in natural jarosite samples from various locations around the world [14–16].

These previous studies did not show how the biomolecules are associated with the jarosite structure. Determination of how the biomolecules are associated with jarosite may provide clues to the stability of the potential signature in the rock record. If the biomolecule is not chemically or physically bound to the mineral structure, it has a greater chance of loss during exposure to harsh weathering environments, thereby, hindering the ability to detect signs of pre-biotic or biotic activity in the geologic record on Earth and other planets. By adding the amino acid breakdown product methylamine (CH_3NH_2) and the amino acid alanine ($C_3H_7NO_2$) to the jarosite synthetic procedure, we sought to determine if a chemical or physical relationship

between the amino acids and the mineral structure could be determined.

The degradation or combustion of methylamine and alanine relate to either biosynthesis or biodegradation by organisms in energy processing pathways [17]. Alanine is important as an intermediate in the formation of more complex amino acids and is integral to biochemical pathways due to its reaction to form pyruvate, an essential molecule in energy pathways such as glycolysis, gluconeogenesis, and the citric acid cycle [18]. Methylamine is linked with the decay of organic matter and is a substrate for methanogenesis [19]. The detection of methane in the martian atmosphere has been suggested as a possible link to biological activity [20–22]. Additionally, alanine is a chiral amino acid; the ratio of one isomer to another could potentially assist in determining a biological origin of the molecule [23]. The detection of either or both of these biomolecules in martian samples could help determine if biological activity ever occurred on Mars.

Very few discussions focus on the abiotic degradation mechanisms of alanine and methylamine except those related to the origins of life on Earth [24, 25]. The mechanisms involve the synthesis of amino acid precursors, such as aldehydes, by a process mimicked in the famous Stanley–Miller volcanic spark experiments [26]. The next step involves the Strecker synthesis of the amino acids by condensation of the aldehyde with ammonium chloride in the presence of potassium cyanide [27]. The reverse reactions (i.e., degradation or combustion) involve the release of methane and ammonia gases and, depending on the environmental conditions, molecular oxygen, hydrogen, and or nitrogen [27, 28].

Thermal analysis techniques are highly sensitive to jarosite composition [29–37], and several studies show that thermogravimetric analysis can differentiate biotic and abiotic samples of calcite and aragonite for astrobiological applications [38, 39]. Herein, we present a thermogravimetric study of the two most stable jarosite group minerals (K-jarosite and Na-jarosite) [40, 41] synthesized in the presence of methylamine and alanine, simple physical mixtures of methylamine and alanine with the jarosites, and the synthetic mineral standards to determine if the physical mixtures, synthesis experiments and mineral standards can be differentiated from one another based on thermal decomposition processes.

Experimental

Syntheses

K-jarosite ($KFe_3(SO_4)_2(OH)_6$) and Na-jarosite ($NaFe_3(SO_4)_2(OH)_6$) were prepared according to the method described in Dutrizac and Chen [42] and also presented in Kotler et al. [14]. Potassium sulfate or sodium sulfate (0.4 M K_2SO_4, Na_2SO_4 were added to a 0.4 M $FeCl_3$ solution in a 100-mL round bottom flask maintaining a stoichiometric ratio of 2:3 sulfate salt to ferric iron during reaction. The solution was stirred under reflux conditions at 100 °C for 24 h. In order to collect the precipitate, the solutions were vacuum filtered while hot using a Buchner funnel and Whatman #4 filter paper. The precipitates were washed under vacuum three times with 1 L of deionized water and air-dried. Synthesis experiments were performed by adding 1 mM concentrations of methylamine (labeled SWMA, synthesized with methylamine) or alanine (labeled SWAla, synthesized with alanine) (Sigma–Aldrich, MA) to the synthesis procedure using the same temperature, time, and washing procedures as the standard jarosite syntheses. Powdered samples were mounted on glass slides for random X-ray powder diffraction analysis to ensure purity and for phase identification. X-ray diffraction analyses were performed on randomly oriented powders using a Philips APD 3720 X-ray diffractometer using a step size of 0.02°2θ and a rate of 0.750°2θ/min. Patterns were compared to jarosite synthetic Joint Committee on Powder Diffraction Standards file 22-0827.

Thermal analysis

Thermal analyses were obtained using a TA Instruments model 2950 thermogravimetric analyzer (TGA). Mixture experiments using methylamine and alanine with synthetic jarosite (jarosite-PMMA and jarosite-PMAla) were prepared by mixing ~3–5% analyte with jarosite matrix before TGA preparations. Sample masses varied between 15 and 20 mg and were heated in a platinum sample holder at a constant ramping of temperature between ambient and 950 °C at a rate of 5 °C/min. Replicate analyses of the K-jarosite standard were performed to assess the reproducibility of the measurements. The standard deviation was calculated to be 0.176 °C/min with a relative standard deviation of 0.45%. All rate calculations and analyses of TGA data were performed using TA Thermal Advantage Universal Analysis (TA Instruments, New Castle, DE, USA) software. Instrument measurements are reported in wt% (elevation in Idaho Falls, ID ≈ 1430 m), however, convention has shifted to report the units as mass%.

Results and discussion

The thermal degradation and derivative mass curves for methylamine and alanine are shown in Fig. 1a–d. Methylamine (CH_3NH_2) (Fig. 1a) begins to degrade at 140 °C, and proceeded through three decomposition steps until the mass loss ceased at 521 °C (see Table 1, Fig. 1a). The derivative mass curve for methylamine (Fig. 1b)

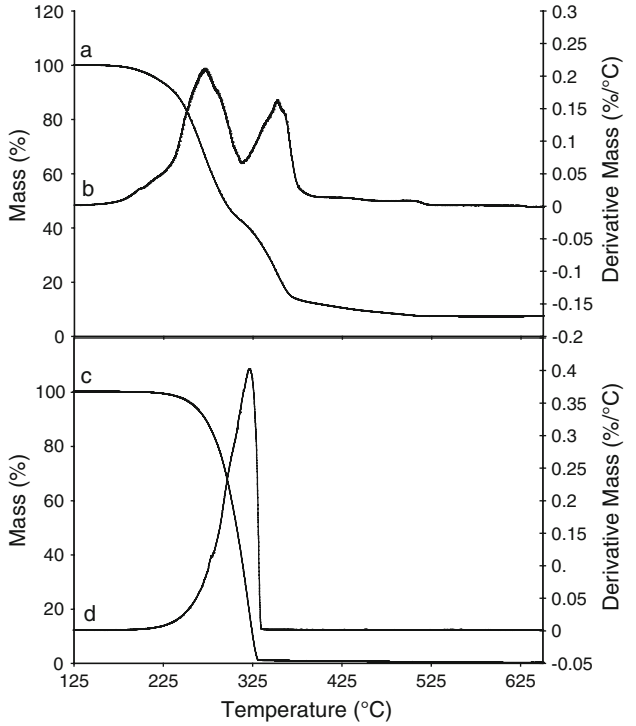

Fig. 1 Thermal degradation and derivative mass curves for methylamine (*a*, *b*) and alanine (*c*, *d*)

shows the presence of two peaks at 270 and 350 °C. Alanine ($C_3H_7NO_2$) begins to degrade at 206 °C, continues through one continuous step until 448 °C, when nearly 100% of the total mass is lost (Fig. 1c, Table 1). The derivative mass curve for alanine (Fig. 1d) shows the presence of a single peak at 320 °C. For the purposes of this discussion, it is the shape of the degradation curves, the onset temperatures, and the presence of indicator peaks within the derivative mass curves that will be compared to the jarosite syntheses and mixture experiment analyses.

Interestingly, when methylamine and alanine are present in physical mixtures with K-jarosite and Na-jarosite (K-jarosite-PMMA, K-jarosite-PMAla, Na-jarosite-PMMA, and Na-jarosite-PMAla), the experiments are conducted to temperatures of 950 °C (Figs. 2, 3). Yet, in all of the methylamine mixture experiments (K-jarosite-PMMA and Na-jarosite-PMAla), the samples regain mass after 750 °C, indicating that the degradation pathway for methylamine likely involves the formation of carbon ash that cannot escape as a gas unlike the alanine degradation in which nearly all the mass is lost as gaseous material. Without the attachment of a gas analyzer to the TGA experimental apparatus, degradation mechanisms and products are speculative.

The thermal degradation and derivative mass curves for the K-jarosite standard (Fig. 2a, b) and Na-jarosite standard (Fig. 3a, b) display distinct decomposition behavior including differences in onset temperature, degradation steps, number of

Table 1 Thermal analysis of methylamine and alanine, K-jarosite and Na-jarosite standard synthetic samples, synthesis and mixture experiments including transition temperatures, total mass loss, and total temperature change (ΔT_{total}) from onset to final

Sample	Step	Transition temperatures (°C)	% original mass
Methylamine (MA)	1	140.02–306.78	44.06
Total mass loss: 92.81%	2	306.78–372.93	13.75
ΔT_{total} = 301.11 °C	3	372.93–521.13	7.18
Alanine (Ala)	1	206.36–331.44	1.23
Total mass loss: 99.62%	2	331.44–447.99	0.38
ΔT_{total} = 241.63 °C			
K-jarosite	1	158.69–317.91	99.71
Total mass loss: 39.22%	2	317.91–418.25	86.94
ΔT_{total} = 646.81 °C	3	418.25–630.64	80.05
	4	630.64–707.40	64.95
	5	707.40–805.02	60.78
K-jarosite-SWMA	1	185.50–319.30	95.73
Total mass loss: 39.38%	2	319.30–425.26	86.00
ΔT_{total} = 603.27 °C	3	425.26–657.92	79.32
	4	657.92–736.63	64.57
	5	736.63–788.77	60.32
K-jarosite-PMMA	1	180.31–412.73	48.15
Total mass loss: 63.81%	2	412.73–768.12	60.32
ΔT_{total} = 587.81 °C			
K-jarosite-SWAla	1	176.25–317.45	95.33
Total mass loss: 39.70%	2	317.45–422.27	85.54
ΔT_{total} = 591.45 °C	3	422.27–557.97	84.31
	4	557.97–644.57	78.99
	5	644.57–724.32	64.46
	6	724.32–767.60	60.28
K-jarosite-PMAla	1	190.27–224.64	97.33
Total mass loss: 50.55%	2	224.64–241.30	86.38
ΔT_{total} = 607.88 °C	3	241.30–420.19	71.03
	4	420.19–653.37	65.56
	5	653.37–745.28	53.10
	6	745.28–798.25	49.45
Na-jarosite	1	251.61–370.97	97.61
Total mass loss: 39.91%	2	370.97–452.51	87.44
ΔT_{total} = 510.41 °C	3	452.51–589.69	84.49
	4	589.69–762.02	60.09
Na-jarosite-SWMA	1	240.12–376.87	97.25
Total mass loss: 39.60%	2	376.87–457.56	87.28
ΔT_{total} = 485.21 °C	3	457.56–590.59	84.72
	4	590.59–725.33	60.48
Na-jarosite-PMMA	1	183.59–376.16	54.23
Total mass loss: 62.64%	2	376.16–607.56	50.43
ΔT_{total} = 558.47 °C	3	607.56–742.06	27.36
Na-jarosite-SWAla	1	244.71–374.03	97.63
Total mass loss: 39.74%	2	374.03–456.96	87.47
ΔT_{total} = 489.89 °C	3	456.96–606.87	84.09
	4	606.87–709.91	60.78
	5	709.91–734.70	60.26
Na-jarosite-PMAla	1	165.12–246.58	93.75
Total mass loss: 43.12%	2	246.58–390.07	90.21
ΔT_{total} = 584.07 °C	3	390.07–450.59	80.83
	4	450.59–642.75	77.50
	5	642.75–749.19	56.88

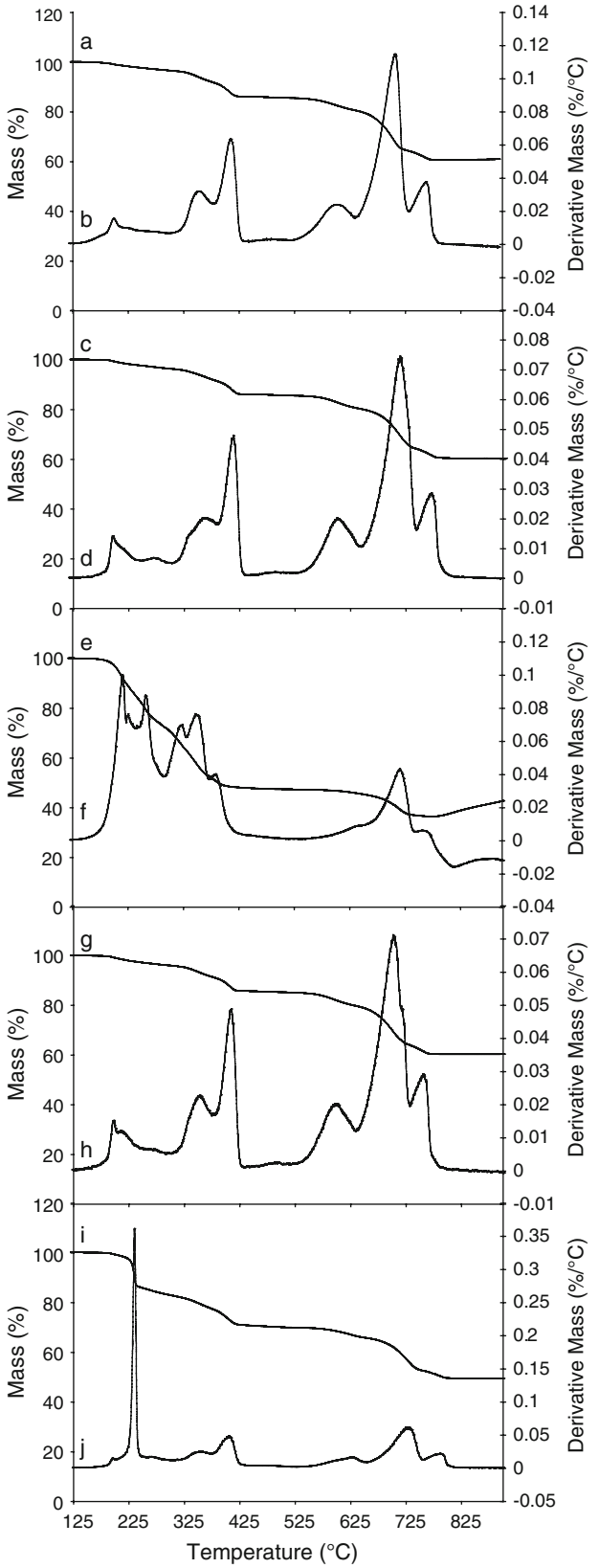

Fig. 2 Thermal degradation and derivative mass curves for K-jarosite (*a*, *b*), K-jarosite-SWMA (*c*, *d*), K-jarosite-PMMA (e, *f*), K-jarosite-SWAla (*g*, *h*), and K-jarosite-PMAla (*i*, *j*)

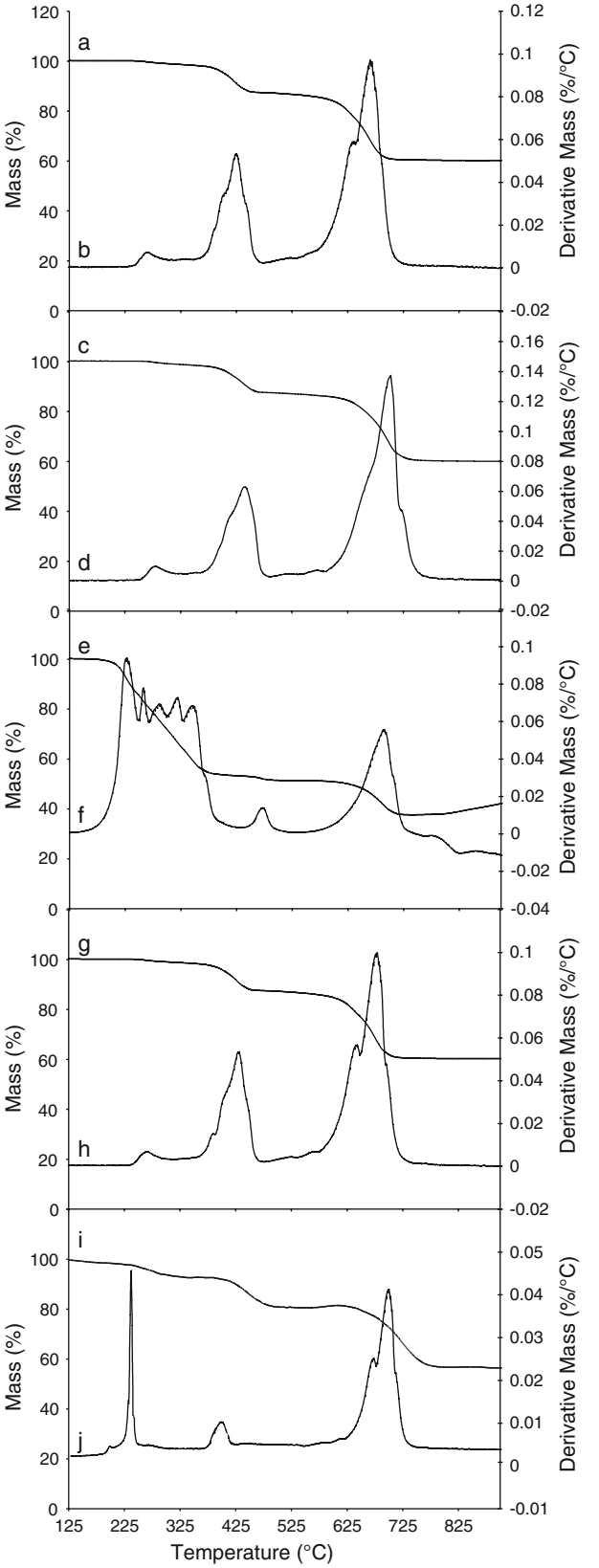

Fig. 3 Thermal degradation and derivative mass curves for Na-jarosite (*a*, *b*), Na-jarosite-SWMA (*c*, *d*), Na-jarosite-PMMA (*e*, *f*), Na-jarosite-SWAla (*g*, *h*), and Na-jarosite-PMAla (*i*, *j*)

derivative mass peaks, and total temperature changes [43]. These experiments show that the K-jarosite and Na-jarosite onset temperatures differ by almost 100 °C (158.69 and 251.61 °C, respectively, Table 1). When the temperatures finally level out (final degradation step), the temperatures for the K-jarosite and Na-jarosite are within 50.0 °C of one another (805.02 and 762.61 °C). In addition to onset temperatures, and final degradation temperatures, the jarosite end members can be distinguished by the number of degradation steps, the number derivative mass peaks and overall shape of the degradation curves (see Figs. 2, 3; Table 1). K-jarosite degrades in five steps with six distinct derivative mass peaks and the Na-jarosite in four steps with only three distinct derivative mass peaks, indicating that composition can be inferred from the thermal degradation and derivative mass curves. It is likely that these differences are directly related to the thermodynamic stability of the two end members. Direct comparison of the $\Delta G_{f,\ 298\ K,\ 1\ bar}$ values for K-jarosite (−3309.8 kJ/mol) and Na-jarosite (−3256.7 kJ/mol) show that free energy of formation values differ by approximately 50 kJ/mol [40, 44].

The K-jarosite-SWMA thermal decomposition and derivative mass curves are shown in Fig. 2c, d. The onset temperature was 185.50 °C, preceded through five steps and mass loss levels out at 788.77 °C (Fig. 2c, Table 1). The number of degradation steps between the K-jarosite and the K-jarosite-SWMA are the same, and qualitatively, the curves appear similar until the K-jarosite-SWMA began to deviate near 600 °C. The derivative mass curve for K-jarosite-SWMA (Fig. 2d) shows a slight shift in the higher temperature peaks, the presence of a diffuse small peak at 270 °C and a small shoulder peak at 350 °C. Both of these additional peaks occur in the indicator region for methylamine (Fig. 1b). The small shoulder peak at 350 °C for K-jarosite-SWMA is likely obscured by the peak for the K-jarosite standard (Fig. 2b) that occurs in the same region.

The K-jarosite-PMMA thermal decomposition curve (Fig. 2e) deviates significantly from both the K-jarosite and K-jarosite-SWMA by degrading in only two steps. The onset temperature is intermediate between K-jarosite and K-jarosite-SWMA at 180.31 °C (Table 1). The derivative mass curve for K-jarosite-PMMA (Fig. 2f) shows several additional peaks in the region where the methylamine indicator peaks should occur. The slight differences between the K-jarosite and K-jarosite-SWMA derivative mass curves indicate that a small quantity of methylamine remained associated with the K-jarosite during the synthesis experiment that can be detected by comparison of the derivative mass curves. It is unknown how much of the methylamine was retained during the synthesis, however a difference is observed between the physical mixture and the synthesis indicating potentially a much lower concentration of methylamine or a different type of association.

The K-jarosite-SWAla thermal degradation and derivative mass curves are shown in Fig. 2g, h. The K-jarosite-SWAla onset temperature was 180.31 °C, the degradation proceeded through six steps, and the final degradation temperature was 767.60 °C (Table 1). The derivative mass curve for K-jarosite-SWAla (Fig. 2 h) is very similar to the K-jarosite with six discernable peaks except that all of the peaks are shifted towards lower temperatures. These results are similar to the K-jarosite-SWMA, which both shows shifts in the degradation curves toward lower temperatures compared to K-jarosite, however there are no sharp distinguishable additional peaks that would indicate the presence of alanine. The K-jarosite-PMAla degrades in six steps with an onset temperature of 190.27 °C. The K-jarosite-PMAla thermal degradation curve (Fig. 2i) mimics the thermal degradation curves of the K-jarosite and K-jarosite-SWAla (Fig. 2a, c) except for the steep initial mass loss (step 1, Table 1), which resembles the degradation curve of alanine alone (Fig. 1c) The K-jarosite-PMAla derivative mass curve (Fig. 2j) is similar to the K-jarosite curve with the addition of a sharp peak at 225 °C. The derivative mass peak for alanine (Fig. 1d) has the indicator peak at 320 °C, however it appears that in the mixture experiments alanine is shifted to lower temperatures indicated by the peak at 225 °C in the K-jarosite-PMAla sample.

The thermal degradation and derivative mass curves for Na-jarosite, Na-jarosite-SWMA, Na-jarosite-PMMA, Na-jarosite-SWAla, and Na-jarosite-PMAla are shown in Fig. 3. The Na-jarosite-SWMA sample began to degrade at 240.12 °C and proceeded through four steps with the final degradation step ending at 725.33 °C (Fig. 3c). The derivative mass curve for Na-jarosite-SWMA (Fig. 3d) shows a shift towards higher temperatures for all three major peaks. There are no peaks in the indicator region where methylamine should occur. Qualitatively, the Na-jarosite and Na-jarosite-SWMA are similar in shape and number of degradation steps. As with the K-jarosite and K-jarosite-SWMA, there is a deviation in behavior where the curves are shifted relative to one another. The Na-jarosite-PMMA degradation curve (Fig. 3e) shows a near perfect match to the K-jarosite-PMMA degradation curve (Fig. 2c), as well as indicator peaks in the methylamine region of the derivative mass curve (Fig. 3f) indicating that, similar to the K-jarosite sample suite, it is possible to distinguish the physical mixture from both the standard and the synthesis experiment samples.

The Na-jarosite-SWAla onset temperature was 244.71 °C, the sample proceeded through five degradation steps and degradation leveled out at 734.70 °C (Fig. 3g, Table 1). Similar to the Na-jarosite-SWMA, the Na-jarosite-SWAla samples showed a shift towards higher temperatures compared to Na-jarosite in both the thermal degradation and

derivative mass curves with no indicator peaks that are representative of either methylamine or alanine. The Na-jarosite-PMAla onset temperature was 165.12 °C and proceeded through five degradation steps with degradation leveling off at 749.19 °C (Fig. 3i). The derivative mass curve for Na-jarosite-PMAla (Fig. 3j) shows the same sharp peak at 225 °C that is observed in the K-jarosite-PMAla derivative mass curve. Similar to the Na-jarosite-PMMA, the Na-jarosite-PMAla shows a shift towards lower temperatures (Figs. 2i, j; 3i, j).

The results of these experiments show that K-jarosites synthesized in the presence of methylamine can be differentiated from each other by small shifts in thermal degradation and derivative mass curves as well as small peaks in the region where methylamine should be present. The physical mixture of methylamine with K-jarosite (K-jarosite-PMMA) can be distinguished by the presence of additional peaks in the derivative mass curve and shifts in temperature for degradation. It is possible that the concentration of methylamine remaining post synthesis is very low and results in only minor changes in the decomposition behavior, but these results indicate that detection is still possible using thermal analysis. For the K-jarosite-SWAla and K-jarosite-PMAla, both samples can be differentiated by their thermal degradation and derivative mass curves from the K-jarosite standard. In all of the K-jarosite experiments with methylamine and alanine, there is a shift towards lower temperatures in the degradation behavior indicating that if methylamine and alanine are present then the samples are less stable and would degrade at a faster rate.

For the Na-jarosite sample suites, Na-jarosite-SWMA can be differentiated from Na-jarosite and Na-jarosite-PMMA. The Na-jarosite-SWMA shows a shift in decomposition behavior towards higher temperatures. For the Na-jarosite alanine experimental suite, only the Na-jarosite-PMAla can be differentiated from the Na-jarosite standard by the presence of an indicator peak at 225 °C, however shifts in temperature indicate for the Na-jarosite-SWAla sample indicate a difference between the sample and the standard. The shifts in temperature for the alanine peak found in the physical mixture is consistent with other thermal analysis results that state the peaks can be shifted dependent upon how the molecule is associated with the sample [45]. The shifts towards higher temperatures would indicate that the structure is more stable and less vulnerable to degradation for the Na-jarosite alanine sample suite.

These results indicate that when biomolecules (i.e., methylamine and alanine) are present in the synthetic procedure for jarosite, their detection and behavior is dependent upon both the jarosite end member and the identity of the biomolecule. Jarosite has been identified as a potential storage molecule for biomolecules in the geologic record [14], and other studies have shown that the crystal structure accommodates a series of atomic and molecular substitutions such as ammonium, hydronium and rare earth elements [46], validating the need to probe the limits of jarosite as a target for identifying evidence of pre-biotic and biotic activity in the geologic record on Earth and other planets. Although thermogravimetric techniques are highly sensitive to composition [47] and have been used to differentiate biotic and abiotic mineralization [38, 39], more sensitive techniques may be better able to detect the small amounts and identify the organic material that may be incorporated in the mineral structure.

Conclusions

The physical mixtures of the biomolecules methylamine and alanine with both K-jarosite and Na-jarosite can be differentiated from one another by thermal analysis, indicating that specific biomolecules can be identified by thermal analysis in these samples. The ability to detect these biomolecules in physical mixtures is important because they may provide information about biological activity related to jarosite. Thermal analysis of both the K-jarosite and Na-jarosite synthesized in the presence of methylamine and alanine show slight differences in their degradation curves compared to the standards, however, only the potassium jarosite synthesized in the presence of alanine and the sodium jarosite synthesized in the presence of methylamine show deviations appreciable enough to make conclusions about their effects on the thermal behavior of the samples. Since jarosite is a target for astrobiological investigations, and both alanine and methylamine are key molecules in biologic processes, these results could prove useful for our exploration of the solar system in the search for life.

Acknowledgements Funding for this research at the University of Montana and the Idaho National Laboratory (INL) comes from the NASA exobiology program (NNX08AP59G). J.M.K. would like to thank the Inland Northwest Research Alliance for graduate support during this project. We would like to thank Christopher Orme of the INL for assistance with thermal analysis. Research performed at the INL under DOE/NE Idaho Operations Office Contract DE-AC07-05ID14517.

References

1. Klingelhofer G, Morris RV, Bernhardt B, Schroder C, Rodionov DS, de Souza PA, et al. Jarosite and hematite at Meridiani Planum from Opportunity's Mossbauer spectrometer. Science. 2004;306(5702):1740–5.
2. Burns RG, editor. Gossans on Mars: spectral features attributed to jarosite. Lun Plan Sci. 1987;XVIII:936–7.
3. Burns RG. Terrestrial analogues of the surface rocks of Mars? Nature. 1989;320:55–6.

4. Akai J, Akai K, Ito M, Nakano S, Maki Y, Sasagawa I. Biologically induced iron ore at Gunma iron mine, Japan. Am Mineral. 1999;84(1–2):171–82.
5. Karamanev DG. Model of the biofilm structure of *Thiobacillus ferrooxidans*. J Biotechnol. 1991;20(1):51–64.
6. Baird AK, Clark BC. Did komatiitic lavas erode channels on Mars? Nature. 1984;311(5951):18.
7. Bibring J, Langevin Y, Mustard JF, Poulet F, Arvidson R, Gendrin A, et al. Global mineralogical and aqueous Mars history derived from OMEGA/Mars express data. Science. 2006;312 (5772):400–4.
8. Bibring JP, Langevin Y, Gendrin A, Gondet B, Poulet F, Berthe M, et al. Mars surface diversity as revealed by the OMEGA/Mars Express observations. Science. 2005;307(5715):1576–81.
9. Burns RG. Terrestrial analogs of the surface rocks of Mars. Nature. 1986;320(6057):55–6.
10. Burns RG. Ferric sulfates on Mars. J Geophys Res [Solid Earth]. 1987;92(B4):E570–4.
11. Burns RG. Iron-sulfur mineralogy of Mars: magmatic evolution and chemical weathering products. J Geophys Res. 1990;95:14415–21.
12. Burns RG. Evolution of sulfide mineralization on Mars. J Geophys Res. 1990;95(B9):14169–73.
13. Burns RG. Rates and mechanisms of chemical weathering of ferromagnesian silicates on Mars. Geochim Cosmochim Acta. 1993; 57:4555–74.
14. Kotler JM, Hinman NW, Yan B, Stoner DL, Scott JR. Glycine identification in natural jarosites using laser desorption Fourier transform mass spectrometry: implications for the search for life on Mars. Astrobiology. 2008;8(2):253–66.
15. Aubrey A, Cleaves HJ, Chalmers JH, Skelley AM, Mathies RA, Grunthaner FJ, et al. Sulfate minerals and organic compounds on Mars. Geology. 2006;34(5):357–60.
16. Skelley AM, Scherer JR, Aubrey AD, Grover WH, Ivester RHC, Ehrenfreund P, et al. Development and evaluation of a microdevice for amino acid biomarker detection and analysis on Mars. Proc Natl Acad Sci USA. 2005;102(4):1041–6.
17. Mathews C, van Holde K, Ahern K. Biochemistry (Benjamin/ Cummings, editor). San Francisco: Addison Wesley Longman; 2000.
18. Umbarger HE. Amino-acid biosynthesis and its regulation. Annu Rev Biochem. 1978;47:533–606.
19. Thauer RK. Biochemistry of methanogenesis: a tribute to Marjory Stephenson. Microbiology. 1998;144:2377–406.
20. Evans J. Exobiology methane could signal life on Mars (Exobiology). Chem Ind. 2009;2:10.
21. Mumma MJ, Villanueva GL, Novak RE, Hewagama T, Bonev BP, DiSanti MA, et al. Strong release of methane on Mars in northern summer 2003. Science. 2009;323(5917):1041–5.
22. Thomas C, Mousis O, Picaud S, Ballenegger V. Variability of the methane trapping in martian subsurface clathrate hydrates. Planet Space Sci. 2009;57(1):42–7.
23. Pizzarello S, Weber AL. Prebiotic amino acids as asymmetric catalysts. Science. 2004;303(5661):1151–4.
24. Chyba C, Sagan C. Electical energy-sources for organic-synthesis on the early Earth. Origins Life Evol Biosphere. 1991;21(1):3–17.
25. Sorrell WH. Interstellar grains as amino acid factories and the origin of life. Astrophys Space Sci. 1997;253(1):27–41.
26. Johnson AP, Cleaves HJ, Dworkin JP, Glavin DP, Lazcano A, Bada JL. The Miller volcanic spark discharge experiment. Science. 2008;322(5900):404–6.
27. Schulte M, Shock E. Thermodynamics of Strecker synthesis in hydrothermal systems. Origins Life Evol Biosphere. 1995;25: 161–8.
28. Simoneit BRT, editor. Prebiotic organic synthesis under hydrothermal conditions: an overview. In – Space Life Sciences – Steps toward origins of life. Adv Space Res. 2004;33(1):88–94.
29. Frost RL, Locke AJ, Martens W. Thermal analysis of beaverite in comparison with plumbojarosite. J Therm Anal Calorim. 2008;92 (3):887–92.
30. Frost RL, Wain D. A thermogravimetric and infrared emission spectroscopic study of alunite. J Therm Anal Calorim. 2008;91 (1):267–74.
31. Frost RL, Weier ML, Martens W. Thermal decomposition of jarosites of potassium, sodium, and lead. J Therm Anal Calorim. 2005;82:115–8.
32. Frost RL, Wills RA, Kloprogge JT, Martens W. Thermal decomposition of ammonium jarosite. J Therm Anal Calorim. 2006; 84:489–96.
33. Frost RL, Wills RA, Kloprogge JT, Martens WN. Thermal analysis of hydronium jarosite. J Therm Anal Calorim. 2006;83 (1):212–8.
34. Hales MC, Frost RL. Thermal analysis of smithsonite and hydrozincite. J Therm Anal Calorim. 2008;91(3):855–60.
35. Ozacar M, Alp A, Aydin AO. Kinetics of thermal decomposition of plumbo-jarosite. J Therm Anal Calorim. 2000;59(3):869–75.
36. Vagvolgyi V, Frost RL, Hales M, Locke A, Kristof J, Horvath E. Controlled rate thermal analysis of hydromagnesite. J Therm Anal Calorim. 2008;92(3):893–7.
37. Vagvolgyi V, Hales M, Martens W, Kristof J, Horvath E, Frost RL. Dynamic and controlled rate thermal analysis of hydrozincite and smithsonite. J Therm Anal Calorim. 2008;92(3):911–6.
38. Stalport F, Coll P, Cabane M, Person A, Gonzalez RN, Raulin F, et al. Search for past life on Mars: physical and chemical characterization of minerals of biotic and abiotic origin: part 1–calcite. Geophys Res Lett. 2005;32(23):L23205.
39. Stalport F, Coll P, Szopa C, Person A, Navarro-Gonzalez R, Cabane M, et al. Search for past life on Mars: physical and chemical characterization of minerals of biotic and abiotic origin. Geophys Res Lett. 2007;34(24):L24102.
40. Baron D, Palmer CD. Solubility of jarosite at 4–35 °C. Geochim Cosmochim Acta. 1996;60:285–95.
41. Navrotsky A, Forray FL, Drouet C. Jarosite stability on Mars. Icarus. 2005;176(1):250–3.
42. Dutrizac JE, Chen TT. Synthesis and properties of V^{3+} analogues of jarosite-group minerals. Can Mineral. 2003;41:479–88.
43. Frost RL, Weier ML, Martens W. Raman spectroscopy of beaverite and plumbojarosite. J Raman Spectrosc. 2005;36(12): 1106–12.
44. Stoffregen RE, Alpers CN, Jambor JL. Alunite-jarosite crystallography, thermodynamics, and geochronology. In: Alpers CN, Jambor JL, editors. Sulfate minerals: crystallography, geochemistry, and environmental significance, reviews in mineralogy and geochemistry, vol 40. Washington, DC: Mineralogical Society of America; 2000. p 453–79.
45. Patron L, Marinescu G, Culita D, Diamandescu L, Carp O. Thermal stability of amino acid-(tyrosine and tryptophan) coated magnetites. J Therm Anal Calorim. 2008;91(1):627–32.
46. Becker U, Gasharova B. AFM observations and simulations of jarosite growth at the molecular scale: probing the basis for the incorporation of foreign ions into jarosite as a storage mineral. Phys Chem Miner. 2001;28(8):545–56.
47. Wendlandt WW. The development of thermal-analysis instrumentation 1955–1985. Thermochim Acta. 1986;100(1):1–22.